6-2011

Investigating the process of fibril formation of the Iowa mutant of the Alzheimer's peptide

Xavier S. Udad
DePaul University, xavier-udad@hotmail.com

INVESTIGATING THE PROCESS OF FIBRIL FORMATION OF THE IOWA MUTANT OF THE ALZHEIMER'S PEPTIDE

By

Xavier S. Udad

B.S., University of Illinois at Chicago, 2001

Research Advisor: Professor Sandra Chimon-Peszek

DISSERTATION THESIS

Submitted as partial fulfillment of the requirements
For the degree of Masters in Chemistry
In the Liberal Arts and Sciences College of
DePaul University, 2011

Chicago, Illinois

To my parents, who have always believed in me.

ACKNOWLEDGEMENTS

I would like to thank Professor Sandra Chimon-Peszek for her guidance, patience, generosity, and beauty; without whom none of this would be possible.

TABLE OF CONTENTS

LIST OF ABBREVIATIONS

Aβ	Beta-amyloid
Aβ1-40	Beta-amyloid Residues 1-40
Aβ22-35	Beta-amyloid Residues 22-35
Aβ WT	Beta-amyloid Wild Type
AD	Alzheimer's Disease
APP	Amyloid Precursor Protein
ATR-FTIR	Attenuated Total Reflectance Fourier Transform Infrared Spectroscopy
CR	Congo Red
D23N	The 23rd amino acid of the beta-amyloid peptide mutated from aspartic acid to asparagine
IOWA	Iowa mutant
IR	Infrared Spectroscopy
ThT	Thioflavine T
UV-Vis	Ultraviolet-Visible Spectroscopy

LIST OF FIGURES

LIST OF TABLES

ABSTRACT

The purpose of this study is to determine how the length of the beta-amyloid peptide, the specific region of the peptide, and a single point mutation affect the behavior of Alzheimer's beta-amyloid. The beta-amyloid peptide, which is a 40 residue peptide that has been implicated as a potential cause of Alzheimer's disease, has been shown to undergo a fibrillization process that involves numerous intermediate stages. One of the intermediate stages has revealed a high neurotoxicity and is believed to be the cause of neurodegeneration associated with Alzheimer's disease. Various point mutations of the beta-amyloid peptide are responsible for the many familial forms of Alzheimer's. Although familial diseases account for only a small percentage of Alzheimer's cases, the study of their behavior can elucidate the mechanism through which fibrillization occurs by determining how each mutation, and its location, affect fibrillization. For the Iowa mutation, residue 23 in the amyloid beta peptide is changed from aspartic acid to asparagine. Residue 23 bonds with residue 28, enabling the peptide to misfold. Although the Iowa mutant undergoes the same general fibrillization process as the wild type, it has a different kinetic profile. This study focuses on a smaller fragment of the beta-amyloid peptide, Aβ22-35, which encompasses the hair-pin turn and the beta-sheet region of the peptide after the hair-pin turn. The point mutation can affect the fibrillization, structure, kinetics, and solubility of the peptide relative to that of the wild type.

CHAPTER 1 - INTRODUCTION

Alzheimer's disease, AD, is the sixth leading cause of death in the United States of America[29]. It is neurodegenerative and the most common form of dementia. It is an incurable, progressive, and terminal disease. AD's advanced stages are characterized by the loss of most/all cognitive and reasoning abilities. Patients no longer recognize people they know or have had lifelong experiences with. They cannot talk, walk, sit, eat, or make sense of the world around them. They must be looked after and cared for twenty-four hours a day, seven days a week[1].

In the early stages, the general symptoms of the disease are short-term memory loss, forgetfulness, and mood swings. As the disease progresses, the symptoms gradually worsen. A person might recognize a loved one one day, not recognize them the next, and recognize them again the day after that. The disease understandably takes an exhaustive toll on those who take care of people with Alzheimer's, as the caregivers are generally those with an emotional attachment to the sufferer[1]. In one particular case study, a 59 year old man had difficulty with reading and driving. He also had problems with locating and identifying items by sight, but his intellect and memory remained intact. As the disease progressed, his memory and language skills eventually deteriorated. An autopsy showed that there was cortical atrophy and a high presence of neurofibrillary tangles and senile plaques[16].

The human brain contains over 100 billion nerve cells, or neurons (Figure 1). These neurons are connected by branches and form an extended network that is responsible for transmitting thoughts, feelings, and memories. It is these neurons that

Alzheimer's disease specifically targets and destroys. As the disease progresses, the size of an Alzheimer's brain continually deteriorates (Figure 2).

Figure 1. An extended network of branched neurons. Image taken from http://www.alz.org/brain/images/05a.jpg.

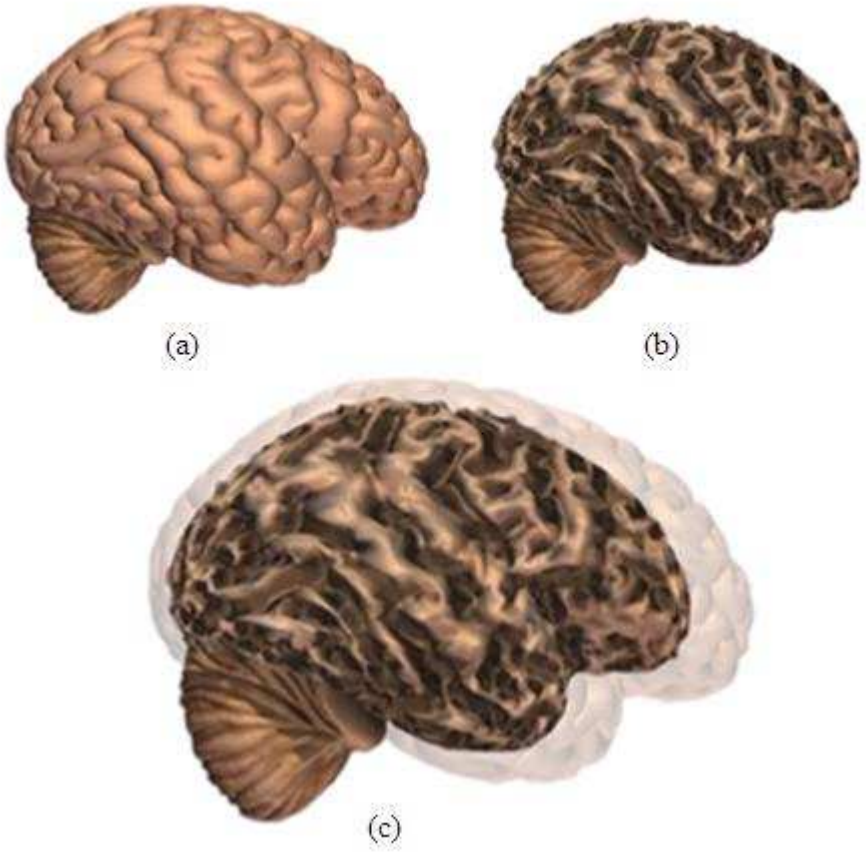

Figure 2. Image of a healthy brain (a) and a diseased brain (b). Both are also juxtaposed for comparison (c). Image taken from http://www.alz.org/brain/images/08_2c.jpg.

The two physical hallmarks of Alzheimer's disease are the presence of tangles and plaques (Figure 3). These are observed whenever autopsies are performed on the brains of those who have died from Alzheimer's. Tangles are made up of twisted strands of tau protein and are found inside dead or dying neurons. Plaques are aggregations of fibril-like structures. Fibrils are long, string-like structures primarily composed of what are commonly referred to as beta-amyloid peptides, or Aβ. And it is the investigation of the beta-amyloid peptide that is the focus of this thesis.

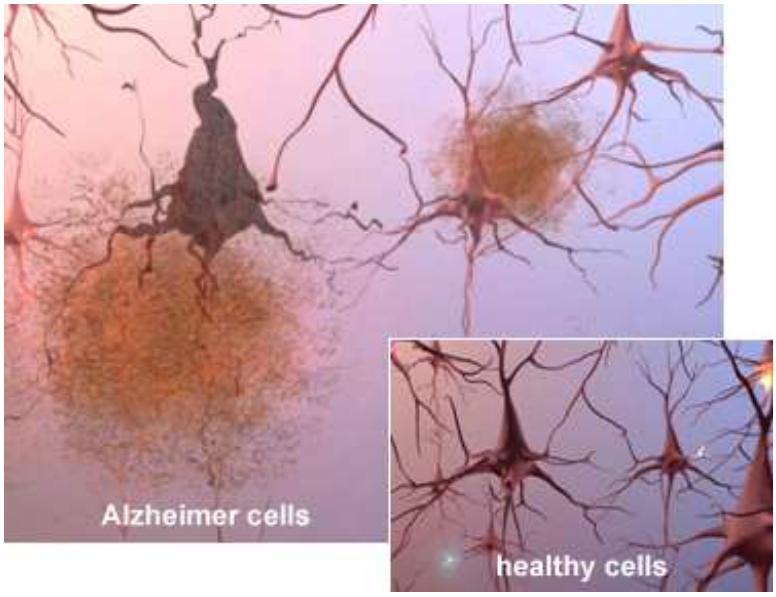

Figure 3. Image of Alzheimer cells with plaques compared to healthy cells. Image taken from http://www.alz.org/brain/images/10d.jpg.

The beta-amyloid attributed to Alzheimer's disease is a peptide that commonly exists as a specific chain of amino acids either 40 or 42 residues in length, and commonly abbreviated as Aβ1-40 or Aβ1-42. The beta-amyloid itself is created by the cleavage of an even larger chain of amino acids known as amyloid precursor protein, or APP. Amyloid precursor protein is found concentrated in the synapses of neurons and its primary function is unknown. Granted, if one were to perform an autopsy and find nothing but fibrils, it would be logical to conclude that it is the fibrils that are responsible for Alzheimer's disease and that it is the fibrils which kill neurons. However, previous studies have shown that a spherical intermediate forms before the fibrillar stage, which is far more toxic than the fibrils themselves, implicating that the intermediate is likely the toxic pathogen for Alzheimer's disease[4,8].

The fibrillization process involves four distinct stages as shown in Figure 4. The first stage is a monomeric random coil with no ordered structure. The second stage is

designated as an intermediate with alpha-helical structure. The third stage is a spherical intermediate with beta-sheet structure. The last stage is the formation of fibrils which also contain said beta-sheets. The change from the second stage intermediate to the third stage intermediate involves a significant morphological transition, namely the formation of well-ordered beta-sheets. There do appear to be other minor stages as well. There is a proto-fibrillar stage that exists between the beta-sheet intermediate and the fibrillar stage. The proposed structure of the beta-sheet intermediate is spherical in nature, with the residues that make up the hair-pin turn being in the center of the structure. Again, it is the spherical beta-sheet intermediate that has experimentally shown itself to be far more toxic than the fibrils[4,8].

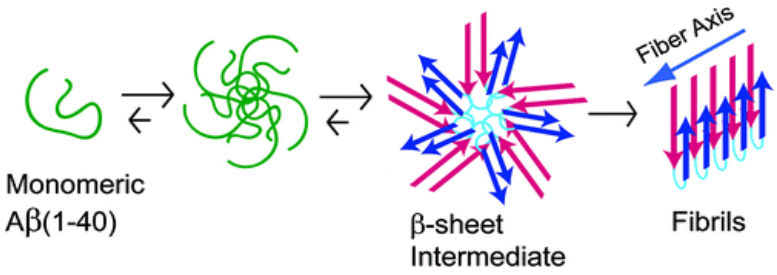

Figure 4. The four main stages of fibrillization[4].

Peptides and proteins are long chains of amino acids; the difference between the two is that proteins are considerably longer. An amino acid consists of an amine, a carboxylic acid, and a substituent group that can vary depending on the structure of the amino acid. Two amino acids can undergo a condensation reaction and form a peptide bond, which releases a molecule of water in the process (Figure 5). From there, it's not

difficult to imagine an entire sequence of amino acids that link up and form peptide chains or even entire proteins.

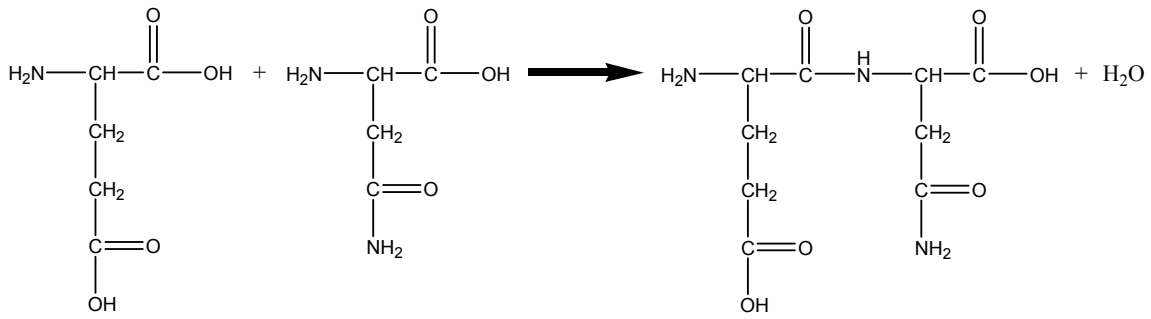

Figure 5. Glutamic acid and asparagine form a peptide bond. Stereochemistry not indicated.

Peptides have four main types of structures. Primary structure is merely the sequence of the acids; the order in which they are bonded together. In the Aβ1-40 peptide, the first amino acid is aspartic acid, the second is alanine, the third is glutamic acid, etc. Secondary structure indicates whether certain sections of the peptide contain one or both structural motifs that are common to biomolecules, namely the alpha-helix and the beta-sheet. Tertiary structure is the three-dimensional shape of the entire peptide, the exact position of each atom relative to other atoms as well as the bond angles between the atoms. Quaternary structure refers to the arrangement of multiple peptides.

An alpha-helix is a chain of amino acids that arrange in a type of spiral configuration (Figure 6). There are both right-handed and left-handed versions and they contain 3.7 residues per turn of the helix. There is also a larger helix that contains 5.1 residues per turn. The twisting peptide chain is held together by hydrogen-bonding. In the helix with 3.7 residues per turn, each amide group is hydrogen bonded to the third

amide group after it along the peptide chain. In the helix with 5.1 residues per turn, each amide group is hydrogen-bonded to the fifth amide group after it[20].

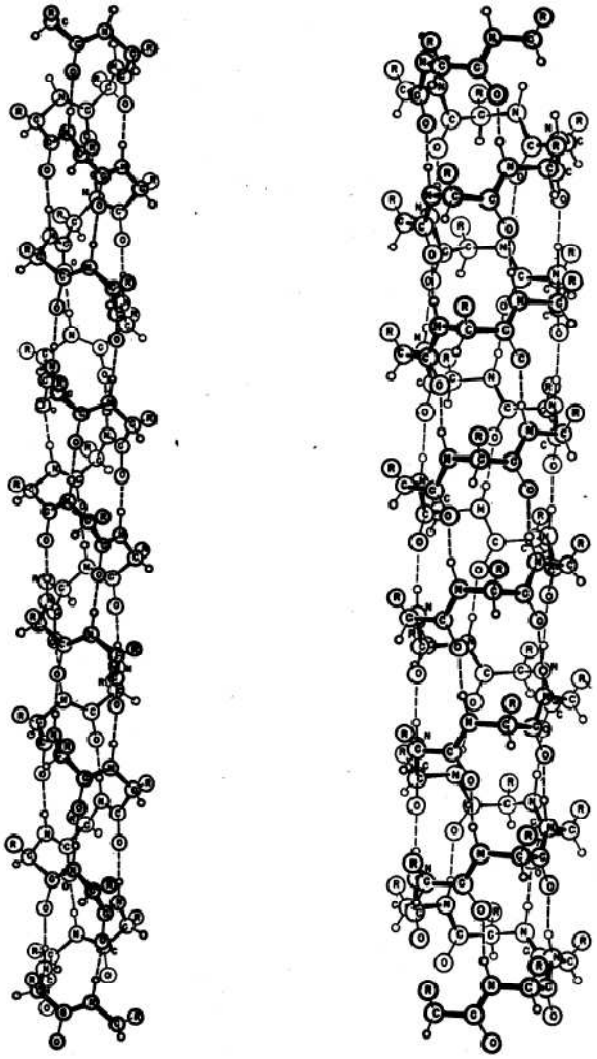

Figure 6. Alpha helices with 3.7 residues per turn and 5.1 residues per turn[20].

Beta-sheets are the other type of secondary structure in biomolecules. The chain of amino acids forms a zig-zagging backbone with alternating carbonyl and amide groups that are also capable of hydrogen-bonding (Figure 7). There are two types of sheets and the main difference between them depends on how the chains are staggered[19]. In a

parallel beta-sheet, the backbone of a peptide chain is lined up with the backbone of another chain. The amine groups, the carbonyls, and the residues are all lined up in such a way that the bends of the backbone of one chain matches up with the bends of another chain. In an antiparallel beta-sheet, the bends are staggered.

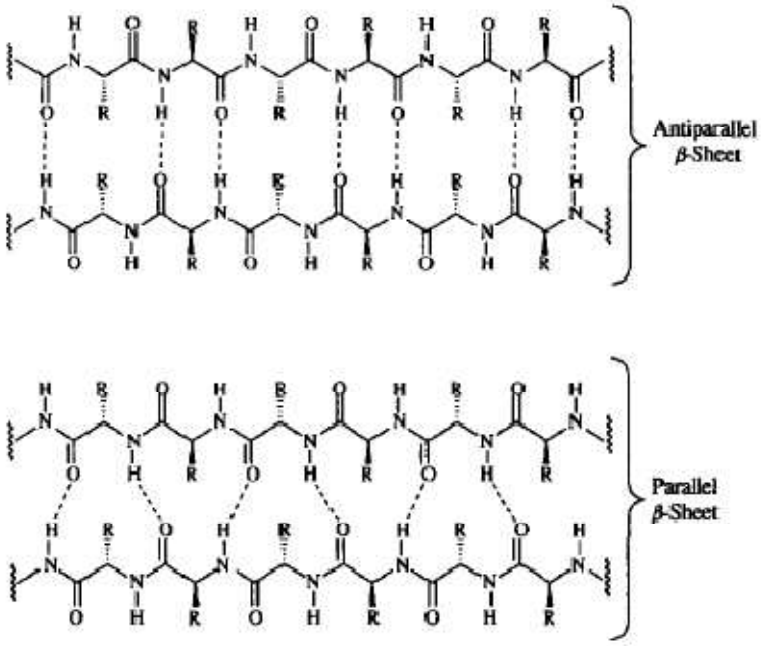

Figure 7. Antiparallel and parallel beta-sheets[19].

Most studies of beta-amyloid focus on Aβ1-40 or Aβ1-42, as these are the fragments that fibrils are primarily composed of. However, studies of smaller fragments are not uncommon and the chemistry of the regions of beta-amyloid have been fairly well mapped out in Figure 8[24].

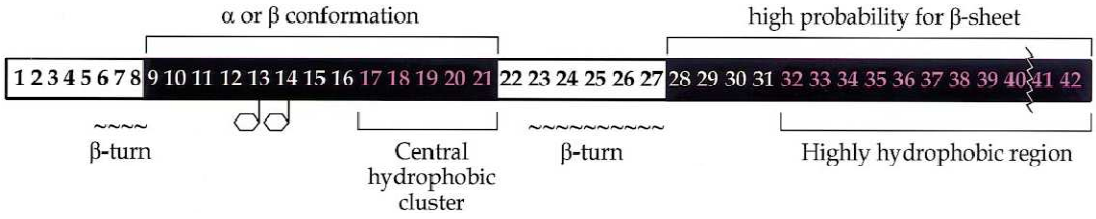

Figure 8. The different regions of beta-amyloid peptide[24].

There are also various strains of Alzheimer's disease that are differentiated based on the type of mutation that the beta-amyloid peptide has. The beta-amyloid wild type, or Aβ WT, is the most frequently expressed form of the peptide that occurs in nature. The Flemish mutation increases the secretion of Aβ peptide, while the Dutch and Iowa mutations enhance fibrillogenesis and the pathogenicity of Aβ[28]. The different strains were named after the geographical region where they were first discovered (Table I).

Mutant strain	Affected peptide	Exists in the wild type as	Mutated to	Abbreviation
Arctic	22	glutamic acid	glycine	E22G
Dutch	22	glutamic acid	glutamine	E22Q
Flemish	21	alanine	glycine	A21G
Iowa	23	aspartic acid	asparagine	D23N
Italian	22	glutamic acid	lysine	E22K

Table I. Mutant strains of Alzheimer's disease[18].

The peptides used for this study are Aβ22-35 WT and Aβ22-35 D23N, a shorter 14 residue fragment with the Iowa mutation. In comparison to the wild type, the Iowa mutation simply expresses asparagine instead of aspartic acid at the 23rd residue and has the following sequence of amino acids:

22 23 24 25 26 27 28 29 30 31 32 33 34 35
H_2N-Glu-**Asn**-Val-Gly-Ser-Asn-Lys-Gly-Ala-Ile-Ile-Gly-Leu-Met-COOH

Residues 22-27 make up the hair-pin turn, 28-35 have a high probability for beta-sheet formation, and residues 32-35 being highly hydrophobic[24]. Different point mutations, like the Iowa mutation, could possibly affect fibrillization and solubility. As this study involved a much shorter residue length (Figure 9), residues 22-35 which is 14 residues in length, its behavior in terms of kinetics and structure were initially an uncertainty.

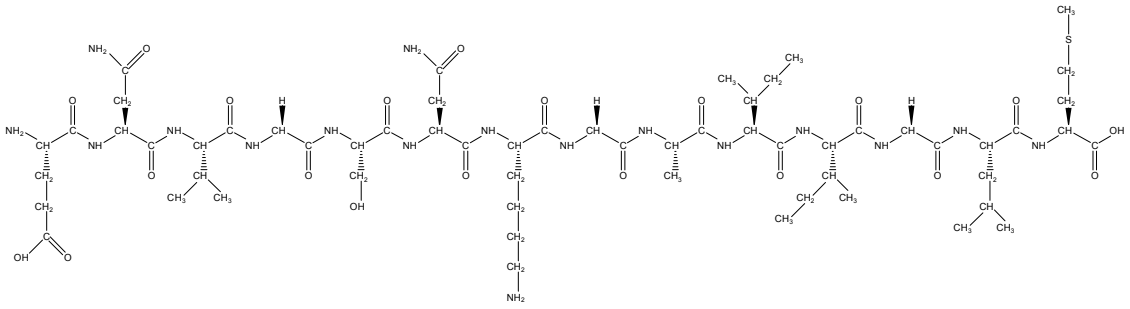

Figure 9. Sequence structure of Aβ22-35 D23N.

In order for all the results to be interpreted properly, comparisons to other studies are necessary. The appropriate peptides for comparison are Aβ1-40 WT, Aβ1-40 D23N, and Aβ22-35 WT. Aβ22-35 D23N is different from the wild type of Aβ1-40 in two

respects, it is shorter and contains a mutation. The full chain, Aβ1-40, is capable of forming intramolecular beta-sheets, whereas this shorter peptide cannot. Any beta-sheets that form from this peptide are likely intermolecular. Any differences between the two peptides could be attributed to either the mutation or the peptide's length. Aβ22-35 D23N is different from Aβ1-40 D23N in only one respect, the length of the peptide. Thus any differences in kinetics or structure could be attributed solely to the peptide's length. Like the full chain of the wild type, the full 1-40 chain of the Iowa mutant is capable of forming both intramolecular beta-sheets and intermolecular beta-sheets. Aβ22-35 D23N is different from Aβ22-35 WT in only one respect, the mutation. Thus any differences in kinetics or structure could be attributed solely to the mutation.

CHAPTER 2 - INSTRUMENTATION

In order to fully characterize the Aβ22-35 D23N peptide, the use of a wide range of bio-analytical instrumentation was necessary. By their nature, peptides can be very difficult to work with for they are non-crystalline. Isolating one stage of the peptide's fibrillization process from the other stages can be arduous as there is always a degree of overlap between the stages. The various techniques used in this study were fluorescence spectroscopy, ultraviolet-visible spectroscopy (UV-Vis), and attenuated total reflectance fourier transform infrared spectroscopy (ATR-FTIR).

2.1 - FLUORESCENCE SPECTROSCOPY

When a molecule absorbs light energy it becomes excited and exists with more energy than it would when it's in its normal ground state; an electron becomes promoted to a higher electronic state. Since the ground state of a molecule is its most stable state, the molecule will attempt to dissipate the extra energy. One of the ways a molecule can do this is to release a photon of light. This is known as fluorescence. Within this higher electronic state there are numerous vibrational states. What is typical of fluorescence in solution is that the excited electron will remain in the higher electronic state, but will relax until it gets down to the lowest vibrational state in the given higher electronic state. This relaxation is possible due to the transfer of energy to surrounding solvent molecules. When the electron gets to the lowest vibrational state in the higher electronic state, it will then release a photon to return to the ground electronic state. Because of relaxation

processes, the photon emission wavelength of fluorescence will be longer than the photon absorption wavelength. And a longer photon wavelength has less energy than a shorter photon wavelength. This is the reason that the emission wavelength of fluorescence is always longer than the absorption wavelength, the molecule absorbs a photon of higher energy but releases a photon of lower energy[7].

The dye molecule Thioflavine T, also known as ThT, is capable of fluorescence and has been shown to quantitatively bind to aggregated beta-sheets. The free dye normally has an absorption wavelength at 385 nm and an emission wavelength at 445 nm. Upon binding to beta-sheet aggregates, the absorption wavelength rises to 450 nm and the emission wavelength rises to 482 nm. This is a unique characteristic of ThT and can be used to correlate the amount of beta-sheet formation with respect to time[16].

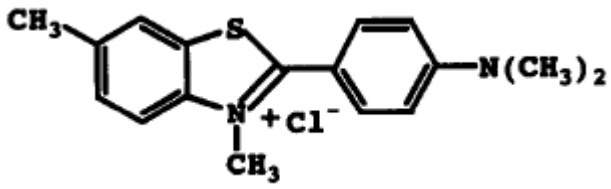

Figure 10. The structure of Thioflavine T[16].

The exact mechanism of ThT binding to fibrils is not known to certainty. However, theoretical models do exist and one such model suggests that ThT binds to the residues of peptides that are in beta-sheet conformation (Figure 11).

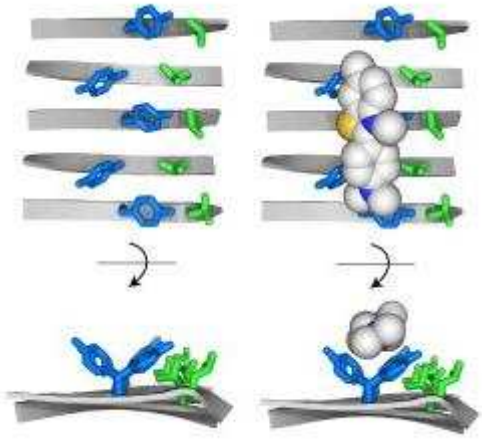

Figure 11. Theoretical model of ThT binding to amyloid fibrils[2].

2.2 - ULTRAVIOLET-VISIBLE SPECTROSCOPY

UV-Vis, ultraviolet-visible spectroscopy, was used to monitor the concentration of Aβ22-35 D23N fibrils. The molecular dye Congo Red was used to quantify beta-sheet formation. A theoretical model of Congo Red binding suggests a ratio of 1 equivalent of Congo Red to 5 equivalents of peptide that have formed an anti-parallel beta-sheet as shown in Figure 12[11].

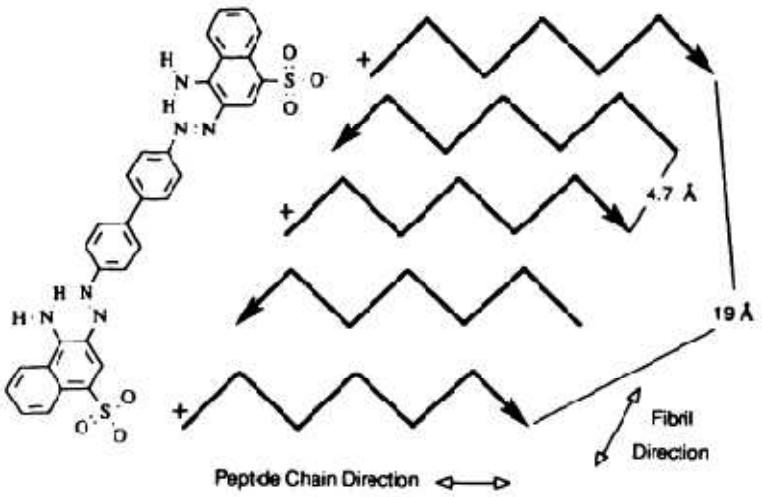

Figure 12. Theoretical binding model of Congo Red to a pentamer of beta-amyloid[11].

The assay itself is a UV-Vis absorbance reading at wavelengths of 403 nm and 541 nm. These wavelengths are unique characteristics of Congo Red when it binds to beta-sheets. An isosbestic point is the specific wavelength at which two chemical species have the same molar absorptivity. The isosbestic point of solutions of varying concentrations of Congo Red is 403 nm. The wavelength of maximum spectral difference between solutions of varying concentrations of Congo Red is 541 nm. Congo Red does not quench and can be used to continually monitor the quantity of beta-sheet formation as it increases over time. The amount of beta-sheet formation due strictly to fibrils can be directly quantified using a modified version of the Klunk equation, an equation that takes the absorbance values at 403 nm and 541 nm and directly correlates them to the amount of amyloid β-peptide aggregation[12].

$$A\beta_{fib} = |({}^{403}A_t/6830) - ({}^{541}A_t/4780) + ({}^{403}A_{CR}/8620)|$$

$A\beta_{fib}$ is the concentration of fibrils in units of molarity. $^{403}A_t$ is the absorbance value at a particular time at 403 nm. $^{541}A_t$ is the absorbance value at a particular time at 541 nm. $^{403}A_{CR}$ is the absorbance value at 403 nm of Congo Red solution prior to the addition of the peptide and is only read once.

2.3 - INFRARED SPECTROSCOPY

When a molecule is exposed to infrared energy, IR, the energy causes the bonds of the molecule to both vibrate and rotate. The wavelengths of light that a substance absorbs in order to vibrate and rotate are unique for each substance, thus every substance has its own unique IR spectrum. The IR spectrum functions as a molecular fingerprint that is just as telling as a human fingerprint. IR can also be used to detect the presence of functional groups as well as provide some indication of structural conformation. A peptide is essentially a chain of amino acids linked by amide bonds. The carbonyl stretching of the amide group, known as the amide I band, generally absorbs itself between 1600 to 1700 cm^{-1}. The shift, or location, of the amide I band gives an indication of secondary structure. If the amide I band is located at 1652-1654 cm^{-1}, this is indicative of an α-helical or unordered structure in solution. If the amide I band is located at 1632-1634 cm^{-1}, this is indicative of β-sheet conformation in solution. Previous studies of synthetic amyloids have demonstrated the amide I band can appear around 1620-1628 cm^{-1} as well[5].

2.4 - ATTENUATED TOTAL REFLECTANCE INFRARED SPECTROSCOPY

Infrared spectroscopy is a standard spectrophotometric technique and sample preparation generally involves the use of salt plates. While the peptide is incubated in a buffer solution with a low concentration of salt, excess salt might cause faster aggregation of the peptide. Any interactions with excess salt could give spectra that is not indicative of the molecule's true structure relative to time. An alternative was necessary, which came in the form of ATR-FTIR. Instead of salt plates, the sample is placed directly on an unreactivde ZnSe crystal. This is very convenient for aqueous solutions as sample preparation is eliminated entirely.

CHAPTER 3 - MATERIALS AND METHODS

3.1 - PHOSPHATE BUFFER SOLUTION

A phosphate buffer solution was made to incubate the peptide. 0.0476 g of Na_2HPO_4 was weighed out and dissolved in 5 mL of Milli-Q water. 0.0456 g of KH_2PO_4 was weighed out and dissolved in another 5 mL of Milli-Q water as well. Milli-Q water is water that has been highly purified and de-ionized by purification systems that are manufactured by Millipore Corporation. The two 5 mL portions were combined and mixed for a total of 10 mL. A quick check with litmus paper showed that the solution was slightly basic and pH adjustment was not necessary. Out of the 10 mL solution, 6.268 mL was measured out. To the 6.268 mL of solution just measured out, 43.732 mL of Milli-Q water was added for a total of 50 mL. A litmus paper check showed this solution was also slightly basic. To the 50 mL solution, 0.00775 g of NaCl and 0.0105 g of NaN_3 were added. The 50 mL solution was the final solution, any remaining or left over solutions were discarded. The last step was simply to filter the 50 mL solution with a 0.22 μm filter. The phosphate buffer solution was 10 mM phosphate buffer, 5 mM NaCl, 0.02% NaN_3.

3.2 BETA-AMYLOID SOLUTION

The target concentration of beta-amyloid peptide in solution was 100 μM. The necessary amount of peptide to attain a 100 μM concentration was dissolved with 0.5 mL

of Milli-Q water then split into a 0.2 mL aliquot and a 0.3 mL aliquot. The 0.2 mL aliquot was diluted to 3 mL with Congo Red solution for beta-sheet formation monitoring via UV-VIS. The 0.3 mL aliquot was diluted to 5 mL with Phosphate Buffer solution for ATR FT-IR. All incubations of the peptide were done at room temperature.

3.3 THIOFLAVIN T SOLUTION

3.7535 g of glycine and 0.16 g of NaOH were weighed out. The two reagents were dissolved together in 900 mL of Milli-Q water. 0.0016 g ThT was weighed out. ThT is reactive to light, therefore precautions were taken to minimize any incident light during the weighing process. The ThT was dissolved with 100 mL of Milli-Q water and transferred to the previously made 900 mL solution of glycine and NaOH. The dissolution and transfer were done with four 25 mL portions of Milli-Q water due to the miniscule amount of ThT.

3.4 - CONGO RED SOLUTION AND UV-VIS

Congo Red solution has the same composition as phosphate buffer solution; 10 mM PBS, 5 mM NaCl, and 0.02% NaN_3; except it also has Congo Red at a concentration of 0.4 μM. The instrument used was a Cary 50 Bio UV-Visible spectrophotometer. The software was package was Varian UV Scan Application, Software Version: 3.00(339). The scan range of the experiment was from 559.0 nm to 397.0 nm and performed at a

temperature of 24^{o}C. Absorbance values at both 541 nm and 403 nm were recorded and substituted into the Klunk equation.

3.5 - ATR-FTIR

The spectrophotometer model used to perform scans was an Avatar 360 FT-IR manufactured by Nicolet. The spectrophotometer was bundled with its own IR software titled *Omnic* version 5.2. The technique used to perform the scans was ATR-IR. This required an additional accessory manufactured by Pike Technologies that housed a ZnSe crystal plate used for ATR-IR. The accessory fit into the scan chamber of the IR in place of standard salt plate holders used for more conventional IR scans. The spectrophotometer was configured under its default settings with the following exceptions: no. of scans set to 32, resolution set to 8, final format set to "% reflectance", correction set to "ATR", gain:8 set to "autogain", accessory set to "avatar multi-bounce", and window material set to "ZnSe". Background scans were performed with the accessory in place. A separate scan of the phosphate buffer solution by itself was taken. The final peptide spectra were the result of subtracting the spectra of the phosphate buffer solution from the spectra of the incubating peptide.

CHAPTER 4 - INITIAL RUNS AND ALTERATIONS

4.1 - THIOFLAVIN T READINGS

Fluorescence readings were performed with a Cary Eclipse fluorescence spectrophotometer manufactured by Varian, Inc. The spectrophotometer was bundled with its own scan application software which was version 1.1(132). The spectrophotometer was configured with the following settings: data mode set to fluorescence, scan setup set to emission, excitation set to 446 nm, start set to 475 nm, stop set to 490 nm, excitation slit set to 5 nm, emission slit set to 5 nm, scan control set to slow, moving average smoothing set to a factor of 5, and PMT detector voltage set to high.

Actual fluorescence readings required establishing an independent blank for each sample, rather than one blank for multiple samples. This was necessary due to quenching by ThT. 980 μL of ThT solution were transferred to a quartz cuvette. The fluorescence value at 482 nm was taken to be the blank value. Samples of incubating peptide for fluorescence readings were prepared by transferring 980 μL of ThT solution into a quartz cuvette, then 20 μL of incubating peptide were transferred to the same cuvette containing the ThT solution. The difference of the fluorescence values of incubating peptide and the blank was taken to be the relative fluorescence.

4.2 - THIOFLAVIN T RESULTS

ThT data revealed no correlation of beta-sheet concentration with regards to time as shown in Figure 13. Absorbance values appear entirely random, and statistical analysis showed no discernable pattern. Previous studies done with Aβ1-40[4], showed a direct and quantifiable rise in β-sheet formation with regards to time.

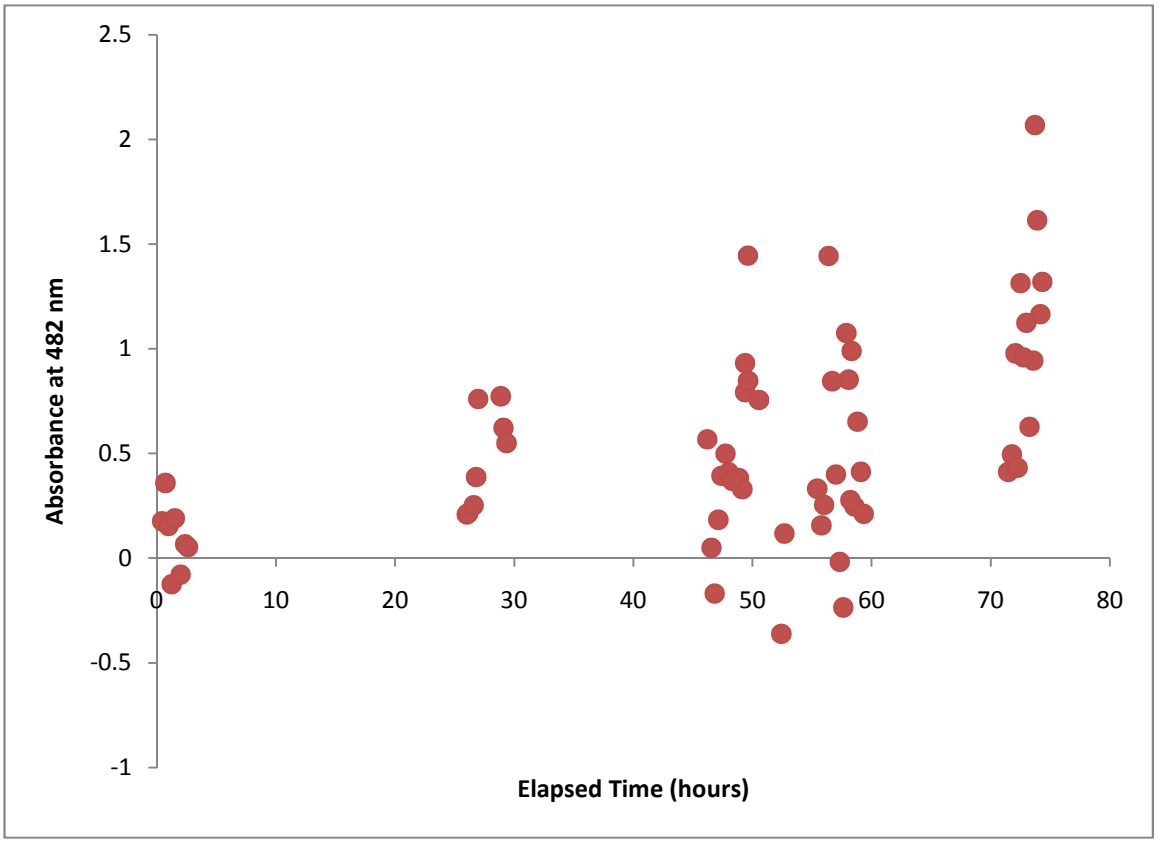

Figure 13. ThT data.

4.3 - MODIFICATIONS MADE AS A RESULT

Due to inconclusive findings, as can be seen from Figure 13, and after extensive research, the decision was made to try new techniques not commonly used for the 22-35 sequence; which led to the thesis project as described in the next chapter.

CHAPTER 5 - SECONDARY STRUCTURE AND FIBRILLIZATION OF THE IOWA MUTANT OF ALZHEIMER'S BETA-AMYLOID 22-35

5.1 - INTRODUCTION

Alzheimer's disease is an irreversible, neurodegenerative disease marked by dementia. The symptoms range from short-term memory loss to mood swings during the early stages; and long-term memory loss, confusion, and withdrawal during the advanced stages[10]. One of its primary physical characteristics is the presence of plaques found in the brains of an affected patient. The plaques are an aggregation of fibril-like structures that are formed by the beta-amyloid peptide[23]. Beta-amyloid, Aβ, is a peptide that can range anywhere from 39 to 43 residues in length. This peptide undergoes a fibrillization process that starts from a monomeric random coil and eventually forms aggregations of fibril-like structures. While the monomer is on its pathway to fibril formation, the peptide forms many intermediates. Though the size of the intermediates vary, they start relatively small and gradually increase in size that are generally spherical in shape[4,8]. One of the intermediates has been shown to have a beta-sheet secondary structural conformation and exhibit toxicity. It is this toxic spherical intermediate, which occurs prior to fibril formation, that is the likely pathogen which causes the neurodegeneration of Alzheimer's disease[4].

The exact mechanisms for fibrillization are not known to certainty, but enough information has been determined to break down the process into a few stages. Based on previous studies performed with the 1-40 residue, the fibrillization process involves four distinct stages. The first stage is a monomeric random coil with no ordered

structure. The second stage is designated as an intermediate which is spherical in shape. The third stage, resembling the second stage in that it is spherical in shape but much larger, exhibits a secondary structure of beta-sheets. The last stage is the formation of fibrils which is also comprised of beta-sheets. There are minor stages in addition tothe four main stages. For instance, there is a proto-fibrillar stage that exists between the β-sheet intermediate and the fibrillar stage. Again, all research up to this point indicates that it is the third stage beta-sheet intermediate that is the most toxic and likely to be the species that is responsible for the actual neurodegeneration of Alzheimer's[4].

The 1-40 peptide itself can be divided into four main regions, with each region having a specific chemistry. Residues 1-8 are random coil, residues 9-21 can form beta-sheets, residues 22-27 make up the hair-pin turn, and residues 28-40 can also form beta-sheets[24]. The rate-determining step for the fibrillization process has been determined to be the folding of the peptide into itself. Residues 23 and 28 form a bond which enables the two beta-sheet regions of the peptide to form an intramolecular beta-sheet, making the chemistry of the hair-pin turn vital to fibrillization[22].

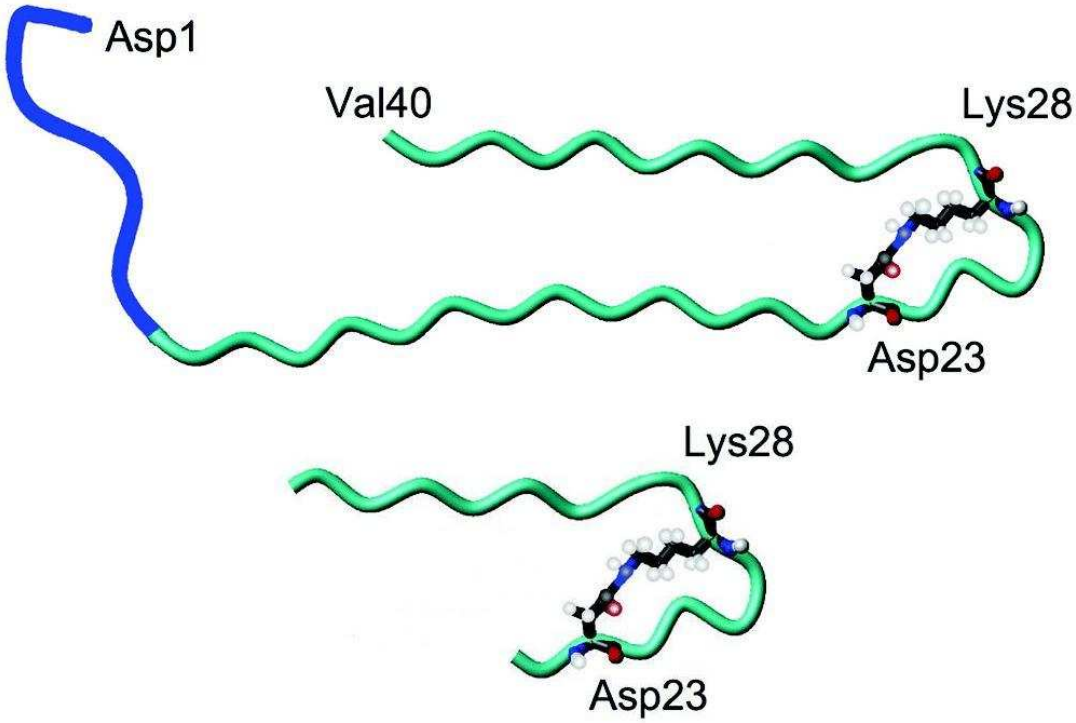

Figure 14. Representations of Aβ1-40 and Aβ22-35[22].

The wild type of beta-amyloid, Aβ WT, is the specific sequence of residues that occurs with the greatest frequency in nature. Point mutations are designated by the wild type residue, the residue where the mutation occurs, and the mutation itself. Thus D23N, the Iowa mutant, indicates that the amino acid has changed from aspartic acid, D, to asparagine, N, on residue 23 (Figure 15). Aβ22-35 D23N means that the 22-35 fragment of beta-amyloid contains the Iowa mutation[27]. This study focuses on two peptides, Aβ22-35 WT and Aβ22-35 D23N. The full chain is 40 residues in length while these smaller fragments are 14 residues in length (Figure 14). Not only are the fragments smaller than the full chain, they also deal with a specific region. Residues 1-14, though the same length as residues 22-35, will behave differently since residues 1-14 are at the beginning of the peptide while residues 22-35 are part of the hair-pin turn. Both regions have

entirely different chemistry[24]. Since smaller fragments are also capable of forming fibrils, they must also form intermediates. The study of smaller fragments is crucial to understanding the minimum peptide length required for fibrillization, as well as determining which regions of the peptide itself are required for fibrillization. So not only is length a consideration, but the specific region of beta-amyloid must be taken into account as well.

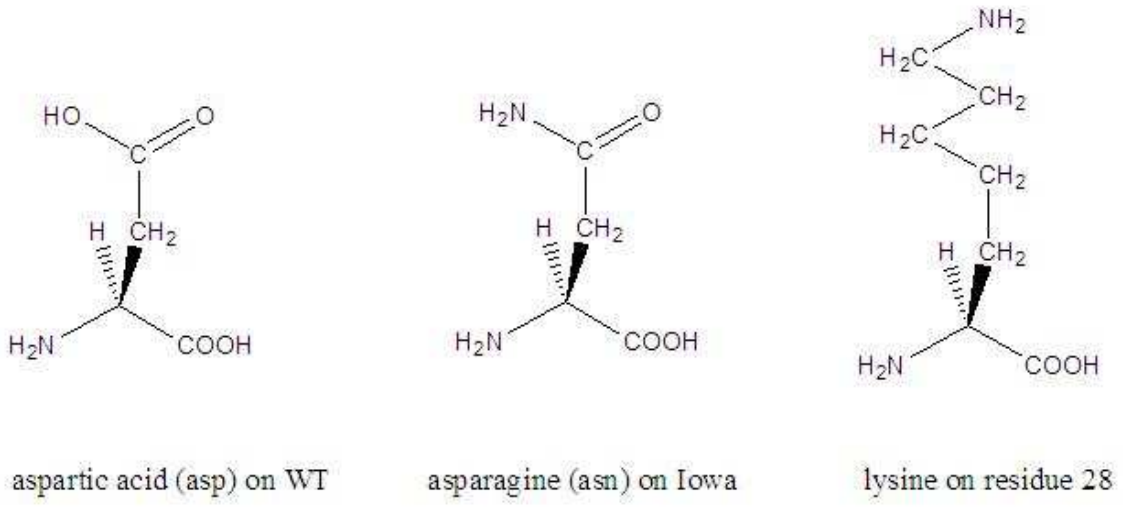

Figure 15. The amino acids on residue 23 of the WT and the Iowa mutant.

The fibrillization process was monitored using two experimental techniques, ATR-IR and UV-Vis via the molecular dye Congo Red. Conventional IR involves the use of salt plates which the peptide, incubated in aqueous solution, can interact with and possibly altering its conformational structure. ATR-IR, attenuated total reflectance, utilizes an unreactive crystal to produce spectra that would be more representative of the peptide's true conformation[3]. The molecular dye Congo Red has characteristic wavelengths when it binds to amyloid beta-sheets. The amount of fibril formation was

monitored with a UV-Vis assay and quantified using a form of the Klunk equation, an equation that takes the absorbance values at 541 nm and 403 nm and directly correlates them to the amount of amyloid β-peptide aggregation:

$$A\beta_{fib} = |(^{541}A_t/4780) - (^{403}A_t/6830) - (^{403}A_{CR}/8620)|$$

$A\beta_{fib}$ is the molar concentration of beta-amyloid fibrils, $^{541}A_t$ is the absorbance value at 541 nm at time t, $^{403}A_t$ is the absorbance value at 403 nm at time t, and $^{403}A_{CR}$ is the absorbance value at 403 nm of Congo Red solution prior to the addition of the peptide. 541 nm is the wavelength of maximal difference between varying concentrations of standard Congo Red solutions. 403 nm is the isosbestic point, which is the wavelength where the absorbances of all the standard Congo Red solutions converge[12].

In order for all the results to be interpreted properly, comparisons to other studies are necessary. The appropriate peptides for comparison are Aβ1-40 WT and Aβ1-40 D23N, both of which have had studies performed on them that are considered to be the standard of reference[4,27]. Aβ22-35 WT is different from Aβ1-40 WT in one respect, it is just a shorter fragment of the larger whole. Any differences in behavior can be attributed solely to the length of the peptide. Aβ22-35 D23N is different from Aβ1-40 WT in two respects, it is shorter and contains a mutation. Differences could either be attributed to the peptide's length or to the mutation. Aβ22-35 D23N is different from Aβ1-40 D23N in only one respect, it is a shorter fragment. Thus any differences could be attributed to the peptide's length. Lastly, Aβ22-35 WT and Aβ22-35 D23N can be compared to each other with any differences being attributed solely to the mutation.

Another significant factor to consider in the fibrillization process is that the full chain, Aβ1-40, is capable of forming intramolecular beta-sheets, whereas these shorter peptides cannot. Any beta-sheets that form from these shorter peptides are likely intermolecular. In the full chain, residues 22-27 make up the hair-pin turn. Residues before the hair-pin and residues after the hair-pin turn can fold into each other and form a beta-sheet self-contained within the same molecule. In addition to intramolecular beta-sheets, Aβ1-40 can also form beta-sheets with other peptides. Aβ22-35, whether WT or D23N, is incapable of forming beta-sheets by folding into itself. Aβ22-35 can only form beta-sheets with other peptides. This fact alone could significantly change the kinetics or the morphology of the fibrillization process of these smaller fragments.

5.2 - RESULTS AND DISCUSSION

5.2.1 - ATR-FTIR ANALYSIS

The current model for fibrillization is a multi-step process that involves significant conformational changes as the peptide progresses from random coil to fibrils. While there are numerous sub-stages, the main stages are random coil, small spherical intermediate, large spherical intermediate with beta-sheet conformation, then lastly, fibrils. The conformation of a single peptide of Aβ1-40 at the fibril stage is a folded, intra-molecular beta-sheet involving the residues preceding the hair-pin turn and the residues after the hair-pin turn, with a bond between residues 23 and 28 enabling the fold. How this conformation itself forms intermolecular beta-sheets with other conformations

in order to nucleate fibrillization is not known. But there are theoretical models, most noteably put forth by the Tycko research group[22]. What is known to certainty is that the basic structure of amyloid fibrils is the continuous stacking of beta-sheets. In this regard, the behavior is quite similar to polymerization.

Another study done by the Tycko group has shown that the folding of the peptide, and its subsequent formation of an intra-molecular beta-sheet, is in fact the rate determining step to fibrillization[22]. The folding is mediated by a bond between residues 23 and 28. The two residues must therefore come into close proximity with each other. This could be facilitated by the peptide adapting an alpha-helical structure prior to forming a beta-sheet. In one type of alpha-helix, the N-H group of one residue forms a hydrogen bond with the C=O group of another residue that is four amino acid units further along the chain. Since residues 23 and 28 are five amino acid units apart, they would come into reasonable proximity if the peptide initially adapted an alpha-helical conformation.

The Aβ22-35 peptide, because of its shortened and truncated nature, is incapable of forming intra-molecular beta-sheets. It lacks the beta-sheet region prior to the hair-pin turn. For shorter peptides that lack beta-sheet regions before or after the hair-pin turn, it would seem that the folding mediated by residues 23 and 28 would not play as crucial a role. However, a bond formed between residues 23 and 28 would in essence create a cyclic "loop" at one end of the peptide chain. This loop could aid, hinder, or affect the fibrillization of a shortened peptide in ways that are very different from Aβ1-40. Because of the steric effect of a loop at one end, the peptide might be forced to fibrillize in one particular way; namely a second peptide forming a beta-sheet with its loop end opposite

to that of the first peptide. The loop end of the shortened peptide of this study is essentially the hair-pin turn of the full peptide, and the hair-pin turn has been shown to be hydrophobic. Since the most economical shape is a sphere, the formation of any spherical species in aqueous solution requires two things, a hydrophobic region and a non-hydrophobic region. Less hindered by mass when compared to the full chain, shortened peptides could form a type of micelle more readily which might lead to the formation of spherical intermediates.

ATR-IR was used to investigate these various conformational changes. The characteristic frequencies at which peptides display intense absorbance peaks have been well documented. The frequencies of the absorbance peaks indicate the secondary structure of the peptide whether it be alpha-helix, beta-sheet, anti-parallel beta-sheet, unordered, or aggregated strands. The two most useful peaks with regards to peptides are the amide I and the amide II peaks. The amide I peak is due to the stretching and vibration of the C=O double bond, while the amide II peak is due to both the C-N and the N-H bond. In general, peptides that have an alpha-helical conformation display amide I and amide II peaks at 1652 to 1657 and 1545 to 1551 cm^{-1} respectively; while peptides that have a beta-sheet conformation display peaks at 1628 to 1635 and 1521 to 1525 cm^{-1}. It should be noted that these values are general guidelines and should not necessarily be held steadfast as several factors contribute to the frequency at which the peaks occur[9].

The IR results, Figure 16, display a gradually increasing intense amide I peak that occurs around 1639 cm^{-1}, which is in reasonable proximity to the amide I peak corresponding to beta-sheets. The intensity of the peak reaches a maximum at 30 hours. The IR results do not show the presence of an amide II peak at all. Due to the peak's

conspicuous absence, no definite conclusion about the peptide's conformation can be reached based on the IR results alone. However, corroborative evidence from a UV-Vis assay does indicate the formation of beta-sheets. This leads to the conclusion that beta-sheet conformation is possible without the presence of the amide II peak, and that the amide I peak alone can be used as a definitive indication of secondary structure. A possible rationalization for the absence of the amide II peak, based on the supposition that the presence of the peak would be due to the vibrations of the bonds, is that the C-N and N-H bonds are already hindered from vibrating. The amide II peak appears for long peptide chains[5]. Shorter peptides are likely to pack more tightly relative to larger peptides. This implies that the vibrations of C-N and N-H bonds are more hindered than the C=O bond for shorter peptides that form beta-sheets.

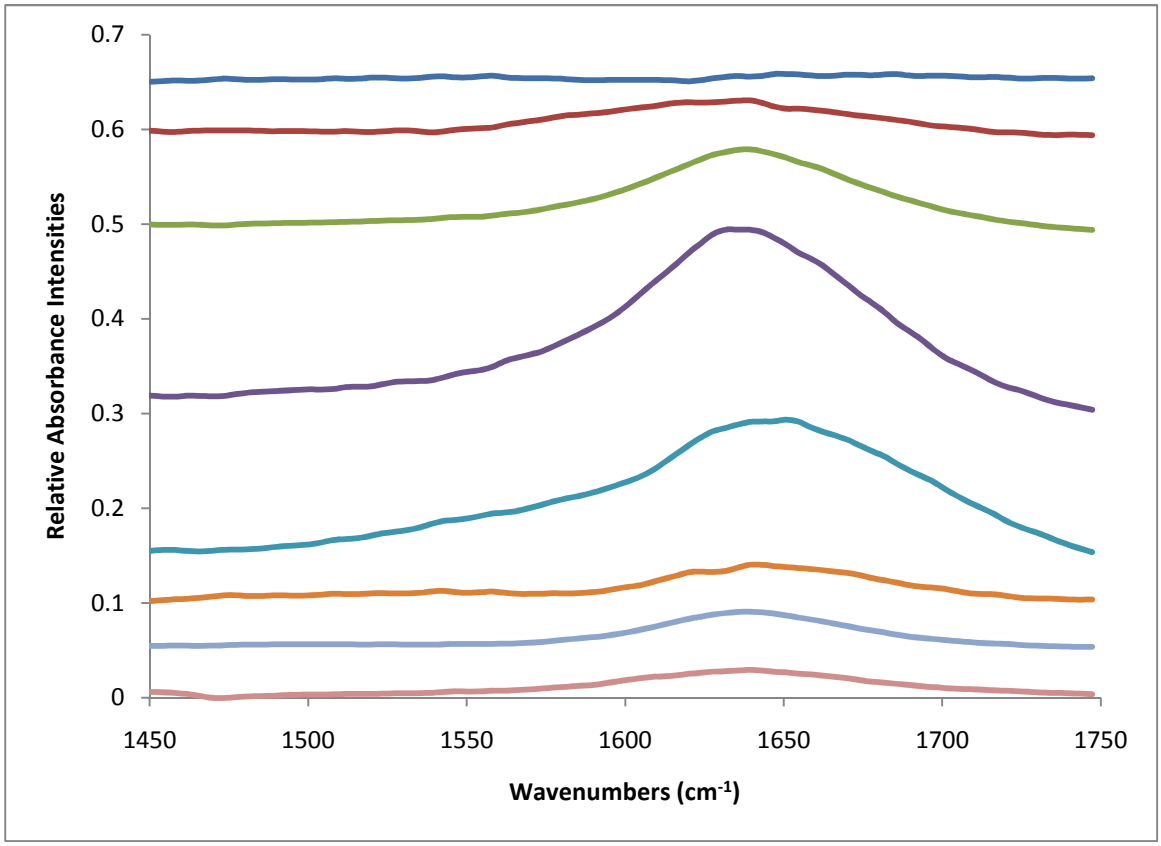

Figure 16. Relative IR profiles of the amide I peak of Aβ22-35 D23N (blue line 0 hours, red line 18 hours, green line 24 hours, purple line 30 hours, turquoise line 36 hours, orange line 42 hours, light blue line 54 hours, pink line 102 hours).

Another crucial aspect of the infrared spectroscopy of the amide I band is the intensity of the absorbance. The amide I peak reaches a maximum intensity at around 30 hours, after 30 hours the intensity gradually decreases. One theory set forth by this study is that this gradual decrease in intensity is an indication of the peptide transitioning from beta-sheet to fibrils. Since infrared spectroscopy involves the stretching and vibration of covalent bonds, the formation of fibrils as beta-sheets continually stack into each other will eventually restrict and hinder the vibrations of covalent bonds. This would result in a decrease of intensity of the amide I peak. With this hypothesis in mind, IR spectroscopy can then be used to detect the transition from secondary structure to tertiary

structure of peptides that can fibrillize. The IR spectra gives no real knowledge of what this tertiary structure is, but it can give an indication of when it starts to occur. IR spectra gave no indication of any type of alpha-helical structure. There is no evidence to suggest that Aβ22-35 D23N initially conforms to an alpha-helix. Although it is entirely possible the transition has a short lifetime and may have simply been missed.

5.2.2 - UV-VIS ANALYSIS

Congo Red is a molecular dye that binds to beta-sheet structures and forms a complex. Direct quantitative measurements of beta-amyloid aggregation can be made with UV-Vis spectroscopy at the characteristic wavelengths of absorbance for this complex. The Aβ22-35 fragment is capable of fibrillization despite the absence of the "KLVFFA" region, which are residues 16-21 of the beta-amyloid peptide. Two types of assays were performed, one with agitation every five hours and one without agitation. The agitation amounted to nothing more than very brief stirring. Both assays show a gradual rise until 30 hours. At 30 hours the rate of fibrillization significantly increases, showing a much steeper slope after 30 hours. 30 hours marks the time of maximum absorbance of the amide I peak in the IR spectra. 30 hours marks the time of the start of fibrillization in the Congo Red assay, further supporting that IR can be used to detect secondary to tertiary transitions of peptides that are capable of fibrillization. The results are shown in Figure 17.

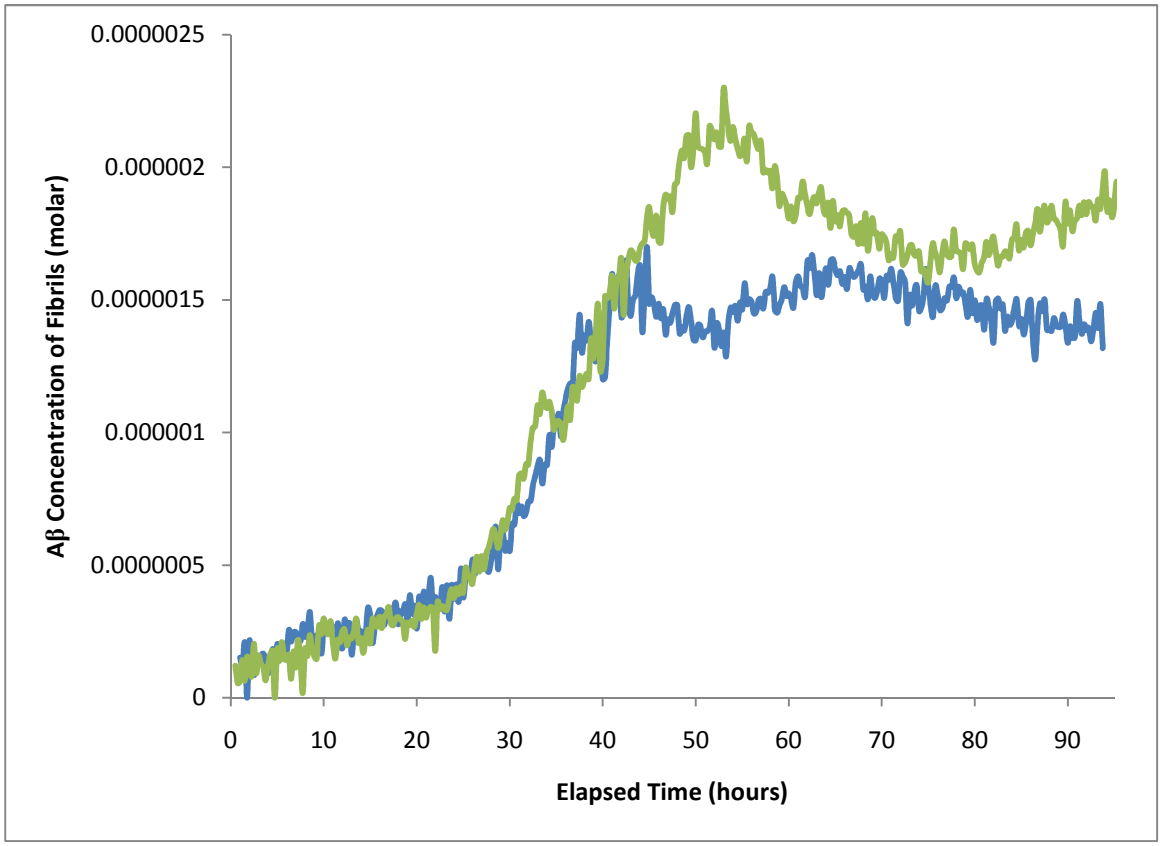

Figure 17. Aβ22-35 D23N molar concentration with respect to elapsed time at 24°C (green line represents brief mixing every 5 hours, blue line represents no mixing).

The assay done with agitation every five hours, green line, reaches a maximum concentration of fibrils at around 53 hours. The assays done with no agitation, blue and red lines, reach a maximum at around 43 hours. This is an indication of when insoluble species start to form, which are likely to be actual fibrils at this stage. Since the fibrils are insoluble, they are affected by gravity and sink to the bottom of the sample system. Any complex formed with the Congo Red and fibrils will not be detected by the UV-Vis spectrometer, and will show a lower concentration of fibrils relative to the assay done with agitation. The plateau indicates that there is some type of equilibrium at 43 hours because its concentration is relatively constant.

5.2.3 - KINETICS AND THERMODYNAMICS

Gibb's free energy, $\Delta G^{\ddagger}$, is an indication of the spontaneity of a reaction and is expressed in terms of enthalpy, $\Delta H^{\ddagger}$, and entropy, $\Delta S^{\ddagger}$.

$$\Delta G^{\ddagger} = \Delta H^{\ddagger} - T\Delta S^{\ddagger} \quad \text{(Equation 1)}$$

The fibrillization process decreases entropy. As more peptides form beta-sheets and start to aggregate, there is less randomness which means $\Delta S^{\ddagger}$ is negative. Since the the formation of fibrils requires the formation of hydrogen bonds, $\Delta H^{\ddagger}$ would have to be negative as well. Strictly speaking, the kinetic profiles for the formation of fibrils are not purely first order. However they can be approximated with first order kinetics up until the plateau is reached. Approximating the fibrillization process with first order kinetics will give a general indication of kinetic and thermodynamic properties. If an exponential regression is performed on the Congo Red assay done without agitation at 24^{o}C (blue line from Figure 17), the kinetic profile, up until the plateau, can be approximated with

$$y = 1 \bullet 10^{-7}\, e^{0.0589x}$$

Therefore k = 0.0589 at 24^{o}C, 24^{o}C is also 297 K. If an exponential regression is performed on the Congo Red assay done without agitation at 40^{o}C, Figure 18,

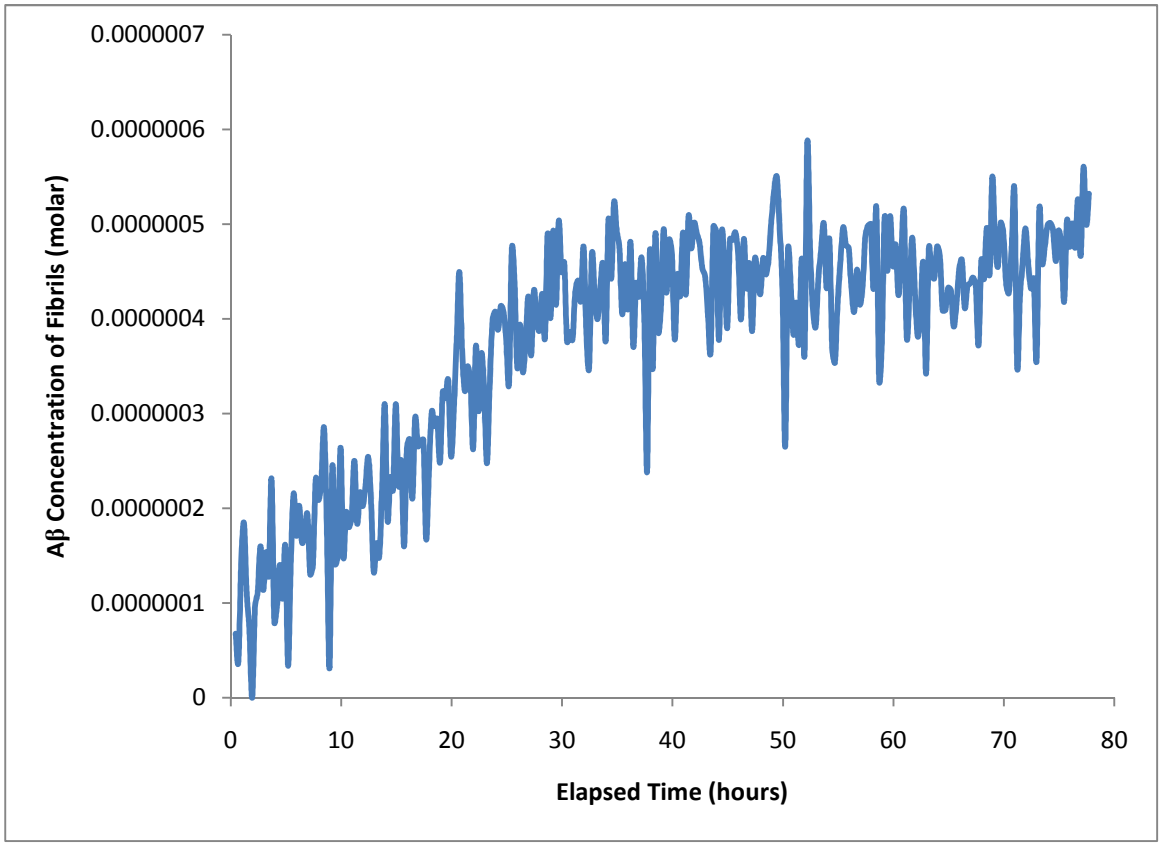

Figure 18. AB22-35D23N molar concentration with respect to elapsed time at 40°C.

the kinetic profile, up until the plateau, can be approximated with

$$y = 1 \bullet 10^{-6}\, e^{0.0529x}$$

Therefore k = 0.0529 at 40°C, which is 313 K.

Gibb's free energy can also be expressed in terms of the rate constant of a reaction.

$$\Delta G^{\ddagger} = -RT \ln k \qquad \text{(Equation 2)}$$

If both expressions for $\Delta G^{\ddagger}$ are set equal, Equation 1 and Equation 2, the following is obtained.

$$-RT \ln k = \Delta H^{\ddagger} - T\Delta S^{\ddagger}$$

When the equation is solved for ln k, the equation takes on a linear form.

$$\ln k = (-\Delta H^{\ddagger}/R)(1/T) + (\Delta S^{\ddagger}/R)$$

$-\Delta H^{\ddagger}/R$ would correspond to the slope of a linear equation and $\Delta S^{\ddagger}/R$ would correspond to the y-intercept. A plot of ln k vs 1/T is shown in Figure 19.

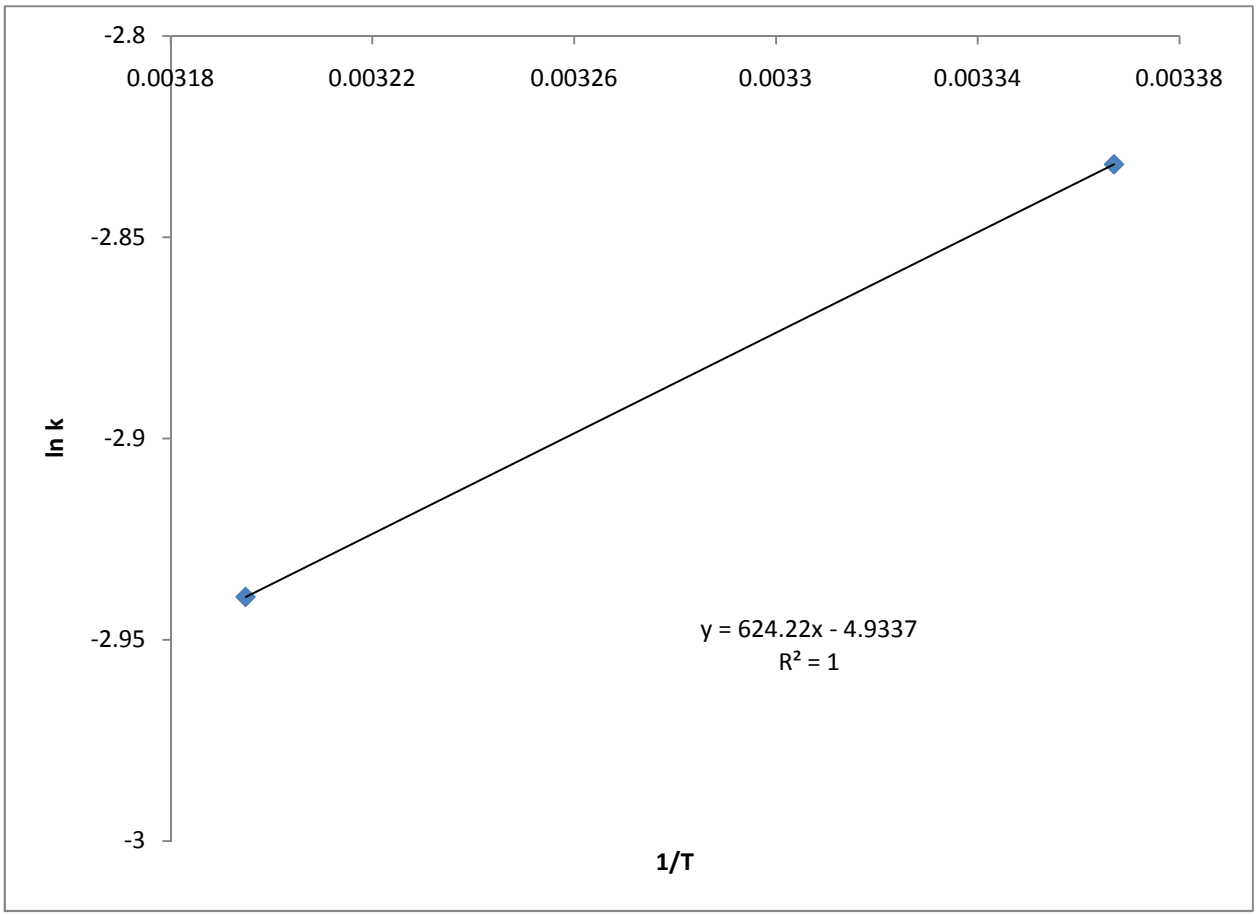

Figure 19. Plot of ln k vs 1/T.

A linear regression performed on a plot of ln k versus 1/T yields the following equation.

$$y = 624.2x - 4.9$$

When these numerical values for slope and y-intercept are set equal to their corresponding factors, both ΔH and ΔS can be calculated.

$$\Delta H^{\ddagger} = -5.2 \text{ kJ/mol}$$

$$\Delta S^{\ddagger} = -41 \text{ J/mol}$$

These values apply only to Aβ22-35 D23N. The magnitudes and signs are as predicted. Using the equation $\Delta G^{\ddagger} = \Delta H^{\ddagger} - T\Delta S^{\ddagger}$ and at a room temperature of roughly 24°C, $\Delta G^{\ddagger}$ = +7.0 kJ/mol; indicating a non-spontaneous reaction. Prior to 30 hours, fibrillization is gradual and slow. At 30 hours, the rate of fibrillization drastically increases. And since the reaction is exothermic, there must be a high activation energy. But once a critical concentration is reached and there is sufficient aggregation, the fibrillization process appears to be self-catalyzing. Sufficient aggregation must therefore lower the activation energy.

5.2.4 - EQUILIBRIUM CONSTANT

Polymerization is the formation of a long chain of a repeating molecular unit via covalent bonding. The fibrillization process is similar to polymerization in that the repeating unit is a peptide and falls under the category of supramolecular polymerization. Supramolecular polymers are defined as polymeric arrays of monomeric units that are brought together by highly directional secondary interactions such as hydrogen bonding, π-π interactions, and hydrophobic interactions[6].

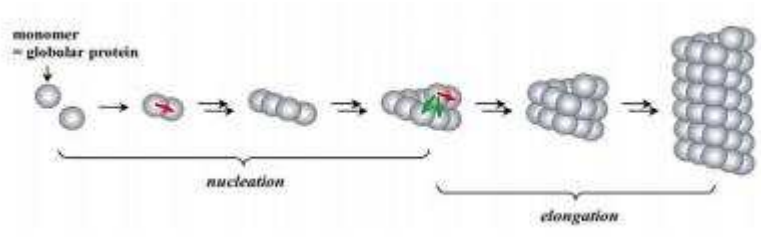

Figure 20. Nucleation-elongation model for supramolecular polymerization[30].

The model used for the calculation of the equilibrium constant of fibrillization is the nucleation-elongation model shown in Figure 20[30]:

$$C_p = \sigma (1 - K[M]) + (1 - \sigma)(1 - K[M])^2 \qquad \text{(Equation 3)}$$

C_p is the concentration of fibrillar species, σ is the nucleation factor, [M] is the concentration of monomeric peptides, and K is the equilibrium constant. For supramolecular polymerization to favor elongation, then $\sigma << 1$. A nucleation factor of 0.0001 was used in these calculations. C_p is the resulting calculation of the Klunk equation, whose parameters are measured experimentally using the Congo Red assay. The relation between [M] and C_p is defined as

$$[M] = [M]_i - 5C_p \qquad \text{(Equation 4)}$$

$[M]_i$ is the initial concentration of monomeric peptide. In all of these experiments, the initial monomeric peptide concentration was 100 μM. The factor of 5 in the second term is due to the theoretical stoichiometric ratio of one molecule of Congo Red binding to five peptides that have formed an extended beta-sheet. The substitution of the expression for [M], equation 4 into equation 3, results in the equation

$$C_p = \sigma\{1 - K([M]_i - 5C_p)\} + (1 - \sigma)\{1 - K([M]_i - 5C_p)\}^2 \qquad \text{(Equation 5)}$$

If this equation (Equation 5) is set to zero, the separate terms of the equation are distributed, and the equilibrium constant factored out from its appropriate term, the resulting equation takes on a quadratic form with respect to the equilibrium constant K.

$$K^2([M]_i - 5C_p)^2(1 - \sigma) + K([M]_i - 5C_p)(\sigma - 2) + (1 - C_p) = 0$$

The standard parameters of a quadratic would result in the following expressions.

$$a = ([M]_i - 5C_p)^2(1 - \sigma)$$

$$b = ([M]_i - 5C_p)(\sigma - 2)$$

$$c = (1 - C_p)$$

The value of the equilibrium constant K can now be determined using the quadratic formula and the data from the green line of Figure 17.

$$K = [-b \pm (b^2 - 4ac)^{1/2}]/(2a)$$

The resulting average value of K was calculated to be 1.1×10^4. This equilibrium constant applies only to Aβ22-35 D23N. The equilibrium constant is not exceedingly high and indicates that there are appreciable amounts of both monomers and products.

5.2.5 - COMPARISON TO Aβ22-35 WT, Aβ1-40 WT, AND Aβ1-40 D23N

The overall fibrillization process is faster for the Iowa mutant than it is for the wild type[21]. Significant fibrillization begins at 30 hours for the Iowa mutant and begins at 40 hours for the wild type. The lag phase occurs at 33 hours for the Iowa mutant and at 46 hours for the wild type. Maximum fibril formation occurs at 53 hours for the Iowa mutant and at 85 hours for the wild type. Despite lacking the ability to form intra-molecular beta-sheets by folding into itself, the hair-pin turn of the 22-35 fragment still somehow plays a significant role in the fibrillization process. If it did not, the kinetic profile of the Iowa mutant and the wild type would be similar. This would suggest that for the fibrillization process to occur, a region of hydrophobicity is required; which the hair-pin turn provides. This would also imply that the folding itself is not as crucial, and that the hair-pin turn simply needs to turn in order to properly coordinate its residues in space to provide a hydrophobic region. Since the shapes of all the intermediates are spherical, the only way for any type of spherical aggregation to be possible is that the species in question has some type of hydrophobic region. And beta-sheets have already been shown to be the predominant conformation of beta-amyloid in fibrils. The minimum requirements for fibrillization would then have to be a hydrophobic region and a beta-sheet region.

Intermediates and fibrils formed from the wild type are probably a mixture of peptides with residue 22 to 28 bonding and residue 23 to 28 bonding. Residues 24 and 25 have no acidic protons; all residue protons are attached to carbon atoms and are non-acidic. A familial mutation at either residue 22 or 23 tends to favor bonding at that

residue. Computer simulations of various mutations show different fibril morphologies based on where the mutation occurs[14], while images of actual fibrils formed from the Iowa mutant show structures that are twisted and untwisted[27]. The Iowa mutant favors the bonding to occur between residues 23 and 28, but there is also likely to be a small percentage of residue 22 to 28 bonding despite the presence of the mutation.

Residues 23 and 28 are the amino acids that bond together and therefore are the most crucial components of the hair-pin turn. In the wild type, residue 23 is aspartic acid. In the Iowa mutant, residue 23 is asparagine. The basic molecular skeletons of aspartic acid and asparagine are the same. They both have a two carbon chain with a double-bonded oxygen attached to the end carbon. The only difference between the two is the other functional group that is attached to the end carbon. In aspartic acid, which is expressed in the wild type, it is –OH. In asparagine, which is expressed in the Iowa mutant, it is $–NH_2$. The Iowa mutation involves the change of a single functional group from –OH to $–NH_2$. This makes the possibility of hydrogen bonding statistically greater for the amine functional group and enabling the peptide to fold sooner.

Comparisons to Aβ1-40 WT and Aβ1-40 D23N are not as straightforward. The definitive studies of the two peptides were performed under slightly different conditions from that of Aβ22-35 D23N[4,27]. In the Aβ1-40 WT study[4], fibrillization was monitored with ThT and the incubation was done at 4^oC. In the Aβ1-40 D23N study[27], incubation of the peptide was done at 37^oC. Nevertheless, logical comparisons can still be made. For the smaller peptide, Aβ22-35, bonding between residues 23 and 28 would logically have to occur sooner than the larger peptide, Aβ1-40. For folding to occur in the larger peptide, peptides 1 to 22 must translate through space, hindering the folding process

entirely with its mass. The absence of peptides 1 to 22 in the smaller peptide should enable the folding process even sooner. Because folding occurs sooner, everything else should occur sooner as well; nucleation, formation of spherical intermediates, fibrillization, etc. Seeding larger peptides with smaller peptides will likely result in faster fibrillization of the larger peptide. It is in this regard, that the region of the peptide plays a crucial role as well. The formation of any spherical species in aqueous solution requires a hydrophobic region and a non-hydrophobic region. If a peptide has no region that is hydrophobic, then spherical intermediates are not likely to form. This further demonstrates just how crucial the hair-pin turn is.

While smaller peptides should logically fibrillize sooner, this doesn't appear to be the case based on the Aβ1-40 WT study[4]. Even though maximum fibrillization occurs at roughly 50 hours for Aβ1-40 WT, this was done at 4^{o}C. At room temperature, maximum fibrillization should occur much sooner. This implies that the longer peptide, Aβ1-40, fibrillizes faster than the shorter peptide, Aβ22-35, at room temperature. This means the formation of an intramolecular beta-sheet lowers the activation energy for the overall fibrillization process more than the formation of intermolecular beta-sheets, despite the fact that the longer peptide has to translate more mass through space in order to form the intramolecular beta-sheet. A peptide shorter than Aβ1-40, with beta-sheet regions before and after the hair-pin turn, would probably fibrillize much faster.

One of the goals of this research is to identify the toxic component of beta-amyloid, to identify which region of the peptide that is responsible for actually killing neuron cells. It is not likely to be the entire peptide, but rather a region of it. Aβ22-35 has only two regions, the hair-pin turn and a beta-sheet region. All research up to this

point indicates that the hair-pin turn is the most crucial region for the fibrillization process, since various mutations in this region affect the peptide's fibrillization rate. Because of its vital role in the fibrillization process, it would stand to reason that it is the hair-pin turn itself that is also likely responsible for neurodegeneration. Toxicity assays done with Aβ22-35 WT have already shown the truncated peptide to be toxic[25]. Toxicity assays done with fibrils have shown the fibrils to be non-toxic relative to the intermediate[8]. It is possible that the structural conversion into beta-sheets is the mechanism responsible for the intermediate's neurotoxicity[4].

The hair-pin turn might play a crucial role in neurotoxicity as well. Both Aβ22-35 WT and Aβ22-35 D23N, cannot form intramolecular beta-sheets. Since these peptides cannot form intramolecular beta-sheets, the hair-pin turn should be of no consequence. And these peptides should have similar if not identical fibrillization rates. Despite this logic, the mutant still fibrillizes faster than the wild type[21]. This means the hair-pin turn is crucial to fibrillization even when intramolecular beta-sheets cannot be formed. A possible future experiment is to incubate only the hair-pin turn which is seven peptides long. If this even shorter peptide forms aggregates and the aggregates are shown to be toxic, then the mechanism of toxicity would be far more complicated than it is believed to be now.

5.3 - SUMMARY AND CONCLUSIONS

While shorter peptides would logically fibrillize faster than longer peptides, this is dependant on the chemistry of the available regions for a shorter peptide. A peptide

shorter than Ab1-40 should fibrillize faster as long as it has a beta-sheet region before and after the hair-pin turn. A shorter peptide with only one beta-sheet region, while still capable of fibrillization, takes much longer to fibrillize than Aβ1-40. The region of the peptide also plays an important role in fibrillization. The minimum requirements for fibrillization are likely to be a hydrophobic region and a beta-sheet region. A hydrophobic region is necessary to form any type of spherical intermediate. A beta-sheet region is necessary for intermolecular interactions to occur in order to form fibrils. The Iowa mutation involves changing aspartic acid to asparagine on the 23rd residue of Alzheimer's beta-amyloid. The molecular skeletons of aspartic acid and asparagine are identical except that aspartic acid has an –OH functional group while asparagine has an –NH_2. There is a greater statistical probability for hydrogen bonding to occur in the Iowa mutant simply because it has one more proton than the wild type. This results in a faster fibrillization process for the Iowa mutant.

REFERENCES

1. Aguerro-Torres H, Fratiglioni L, Winblad B (1998) Natural History of Alzheimer's Disease and Other Dementias: Review of the Literature in the Light of the Findings from the Kungsholmen Project. *International Journal of Geriatric Psychiatry* Vol 13: 755-766

2. Biancalana M, Koide Shohei (2010) Molecular mechanism of Thioflavin-T binding to amyloid fibrils. *Biochimica et Biophysica Acta* Vol 1804, Issue 7: 1405-1412

3. Cerf E, Sarroukh R, Tamamizu-Kato S, Breydo L, Derclaye S, Dufrenes Y, Narayanaswami V, Goormaghtigh E, Ruysschaert J, Raussens V (2009) Antiparallel β - sheet: a signature structure of the oligomeric amyloid β-peptide. *Biochemical Journal* Vol 421: 415-423

4. Chimon S, Shaibat M, Jones C, Calero D, Aizezi B, Ishii Y (2005) Evidence of fibril-like β-sheet structures in a neurotoxic amyloid intermediate of Alzheimer's beta-amyloid. *Natural Structure & Molecular Biology* Vol 14: 1157-1164

5. Choo L, Wetzel D, Halliday W, Jackson M, LeVine S, Mantsch H (1996) In Situ Characterization of β-Amyloid in Alzheimer's Diseased Tissue by Synchrotron Fourier Transform Infrared Microspectroscopy. *Biophysical Journal* Vol 71: 1672-1679

6. De Greef T, Smulders M, Wolffs M, Schenning A, Sijbesma R, Meijer E (2009) Supramolecular Polymerization. *Chemical Reviews* Vol 109: 5687-5754

7. Hercules D (1966) *Fluorescence and Phosphorescence Analysis* John Wiley & Sons Inc, New York

8. Hoshi M, Sato M, Matsumoto S, Noguchi A, Yasutake K, Yoshida N, Sato K (2003) Spherical aggregates of β-amyloid (amylospheroid) show high neurotoxicity and activate tau protein kinase I/glycogen synthase kinase-3β. *Proceedings of the National Academy of Sciences* Vol 100, No 11: 6370-6375

9. Jackson M, Mantsch H (1995) The Use and Misuse of FTIR Spectroscopy in the Determination of Protein Structure. *Critical Reviews in Biochemistry and Molecular Biology* Vol 30, No 2: 95-120

10. Jost B, Grossberg G (1996) The evolution of psychiatric symptoms in Alzheimer's disease: a natural history study. *Journal of the American Geriatrics Society* Vol 44, No 9: 1078-1081

11. Klunk W, Pettegrew J, Abraham D (1989) Quantitative Evaluation of Congo Red Binding to Amyloid-like Proteins with a Beta-pleated Sheet Conformation. *Journal of Histochemistry and Cytochemistry* Vol 37, No 8: 1273-1281

12. Klunk W, Jacob R, Mason R (1999) Quantifying Amyloid β-Peptide (Aβ) Aggregation Using the Congo Red-Aβ (CR-Aβ) Spectrophotometric Assay. *Analytical Biochemistry* Vol 266: 66-76

13. Krebs M, Bromley E, Donald A (2005) The binding of thioflavin-T to amyloid fibrils: localization and implications. *Journal of Structural Biology* Vol 149, Issue 1: 30-37

14. Krone M, Baumketner A, Bernstein S, Wyttenbach T, Lazo N, Teplow D, Bowers M, Shea J (2008) Effects of familial mutations on the folding nucleation of the Alzheimer Amyloid β-protein. *Journal of Molecular Biology* Vol 381, No 1: 221-228

15. Kusumoto Y, Lomakin A, Teplow D, Benedek G (1998) Temperature dependence of amyloid β-protein fibrillization. *Proceedings of the National Academy of Sciences* Vol 95: 12277-12282

16. LeVine H (1993) Thioflavine T interaction with synthetic Alzheimer's disease β-amyloid peptides: Detection of amyloid aggregation in solution. *Protein Science* Vol 2, Issue 3: 404-410

17. Levine D, Lee J, Fisher C (1993) The visual variant of Alzheimer's disease. *Neurology* Vol 43: 305

18. Murakami K, Irie K, Morimoto A, Ohigashi H, Shindo M, Nagao M, Shimizu T, Shirasawa T (2002) Synthesis, aggregation, neurotoxicity, and secondary structure of various Aβ1-42 mutants of familial Alzheimer's disease at positions 21-23. *Biochemical and Biophysical Research Communications* Vol 294, No 1: 5-10

19. Nesloney C, Kelley J (1996) Progress Towards Understanding β-Sheet Structure. *Bioorganic & Medicinal Chemistry* Vol 4, No 6: 739-766

20. Pauling L, Corey R, Branson H (1951) The Structure of Proteins: Two Hydrogen-bonded Helical Configurations of the Polypeptide Chain. *Proceedings of the National Academy of Sciences* Vol 37, No 4: 205-211

21. Reinsalu S, Rohn E, Chimon-Peszek S

22. Sciarretta K, Gordon D, Petkova A, Tycko R, Meredith S (2005) Aβ40-Lactam(D23/K28) Models a Conformation Highly Favorable for Nucleation of Amyloid. *Biochemistry* Vol 44: 6003-6014

23. Selkoe D (2004) Cell biology of protein misfolding: The examples of Alzheimer's and Parkinson's diseases. *Nature Cell Biology* Vol 6, No 11: 1054-1061

24. Serpell L (2000) Alzheimer's Amyloid Fibrils: Structure and Assembly. *Biochimica et Biophysica Acta* Vol 1502: 16-30

25. Takadera T, Sakura N, Mohri T, Hashimoto T (1993) Toxic effect of a β-amyloid peptide (β22-35) on the hippocampal neuron and its prevention. *Neuroscience Letters* Vol 161: 41-44

26. Timasheff S, Susi H, Stevens L (1967) Infrared Spectra and Protein Conformations in Aqueous Solutions. *Journal of Biological Chemistry* Vol 242, No 23: 5467-5473

27. Tycko R, Sciarretta K, Orgel J, Meredith S (2009) Evidence for Novel β-Sheet Structure in Iowa Mutant β-Amyloid Fibrils. *Biochemistry* Vol 48: 6072-6084

28. Van Nostrand W, Melchor J, Cho H, Greenberg S, Rebeck G (2001) Pathogenic Effects of D23N Iowa Mutant Amyloid β-Protein. *The Journal of Biological Chemistry* Vol 276, No 35: 32860-32866

29. Xu J, Kochanek K, Murphy S, Tejada-Vera B (2010) *National Vital Statistics Report* Vol 58, No 19

30. Zhao D, Moore J (2003) Nucleation-elongation: a mechanism for cooperative supramolecular polymerization. *Organic and Biomolecular Chemistry* Vol 1: 3471-3491

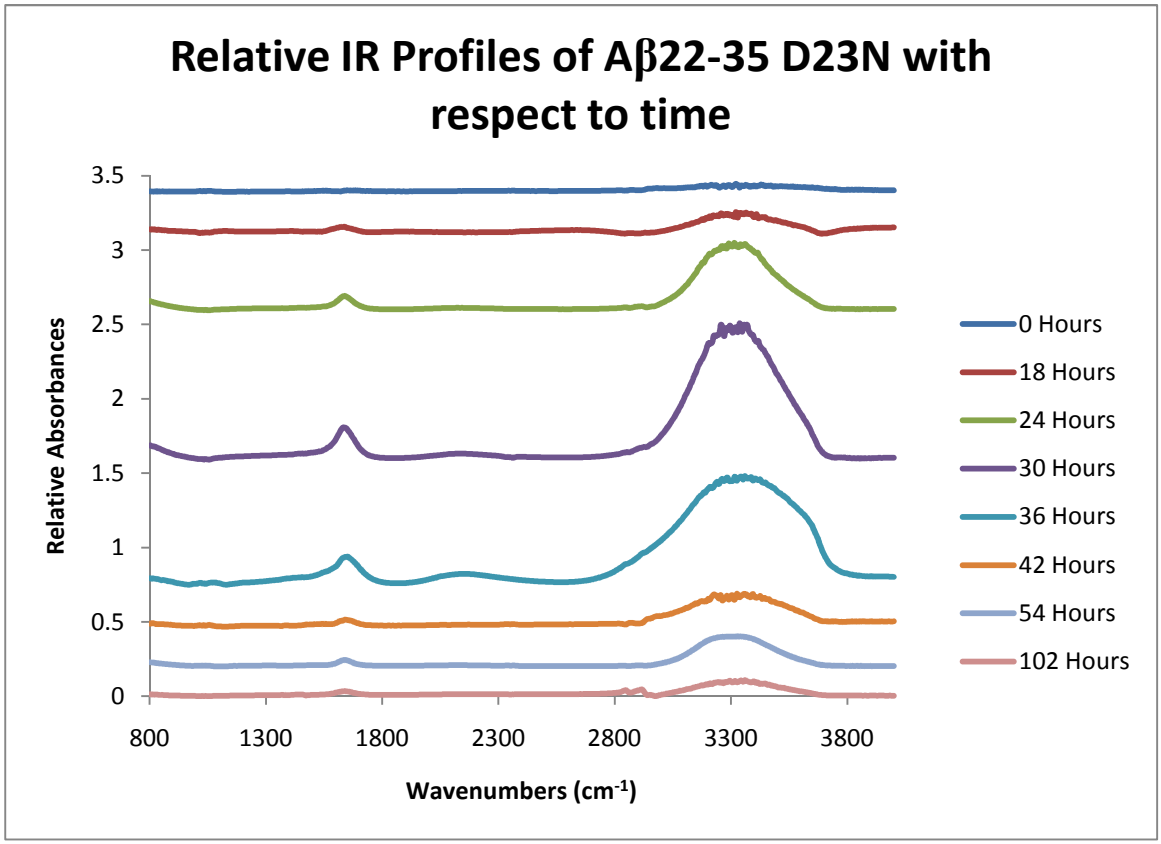
Relative IR Profiles of Aβ22-35 D23N with respect to time
Relative Absorbances
3.5
3
2.5
2
1.5
1
0.5
0
800
1300
1800
2300
2800
3300
3800
Wavenumbers (cm-1)
0 Hours
18 Hours
24 Hours
30 Hours
36 Hours
42 Hours
54 Hours
102 Hours

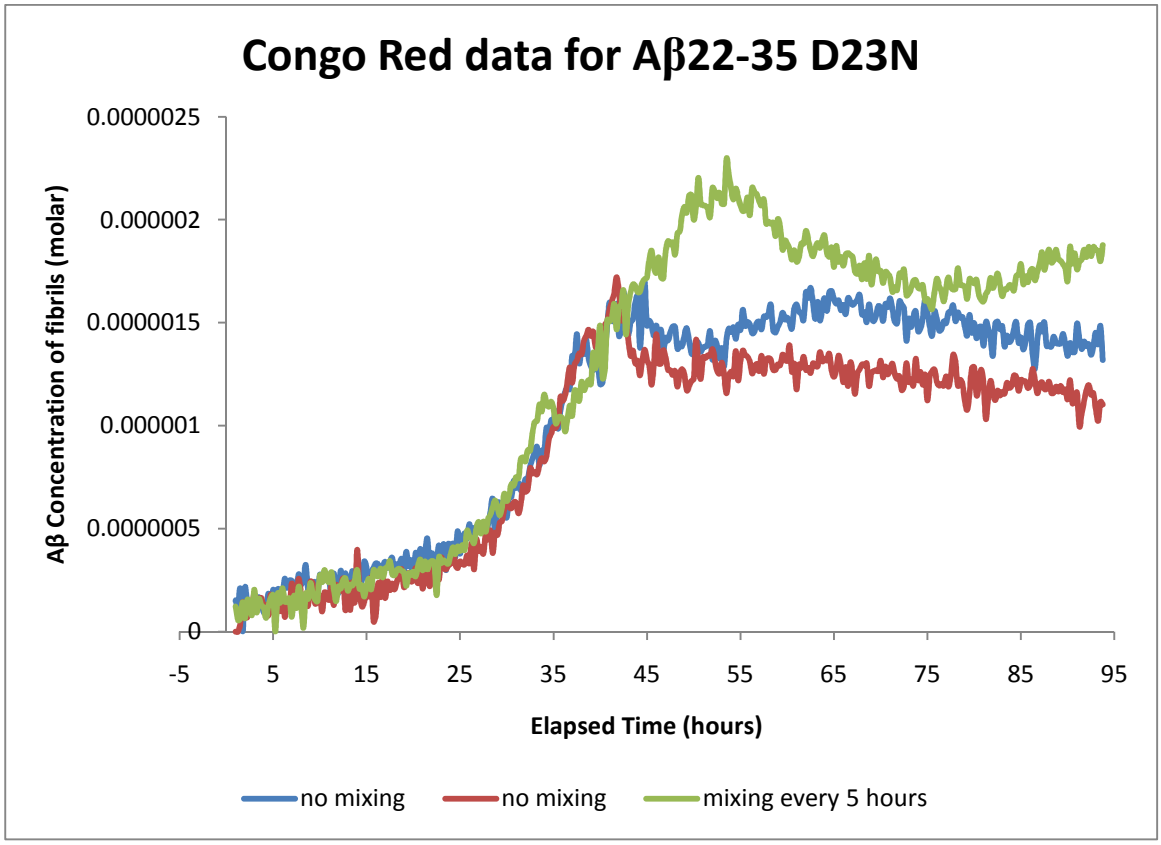
Congo Red data for Aβ22-35 D23N
Aβ Concentration of fibrils (molar)
0.0000025
0.000002
0.0000015
0.000001
0.0000005
0
-5
5
15
25
35
45
55
65
75
85
95
Elapsed Time (hours)
no mixing
no mixing
mixing every 5 hours